Limited long-term cooling effects of flood basalt emplacements

Jack Longman[1,2,*], Benjamin J.W. Mills[3], Andrew S. Merdith[3,4]

[1]Department of Geography and Environmental Sciences, Northumbria University, Newcastle upon Tyne, United Kingdom

[2]Marine Isotope Geochemistry, Institute for Chemistry and Biology of the Marine Environment (ICBM), University of Oldenburg, Oldenburg, Germany

[3]School of Earth and Environment, University of Leeds, Leeds, UK.

[4]School of Physics, Chemistry and Earth Sciences, University of Adelaide, Adelaide, Australia

[*] Corresponding author: jack2.longman@northumbria.ac.uk

This manuscript has been submitted for publication in *PNAS* and is currently under review. This version of the manuscript has not been peer reviewed.

Abstract

The emplacement of large igneous provinces (LIPs) is known to have been a driver of climate change in Earth's past, particularly during the breakup of Pangaea. However, the balance between climate warming through CO_2 emission and climate cooling through increased weathering is poorly understood. To better understand the role of LIP emplacement on long-term climate change, we utilize a coupled climate-biogeochemical model which considers the holistic impact of LIPs through both degassing of CO_2 and enhancement of local continental weathering rates. Of the 7 LIPs during the breakup phase of Pangea (approximately between 300 and 150 Ma), only the Central Atlantic Magmatic Province (CAMP) drives long-term cooling in our model, and this is a minor effect despite emplacement of a very large surface area in the humid tropics. Similarly, only the CAMP imparts a clear stepwise change in the long-term strontium isotope record whereas the other LIPs of this period do not. Due to relatively small areal extents, and emplacement often outside the tropical weathering zone, we conclude that most LIPs have no significant global cooling effect on multimillion year timescales.

Significance Statement

Large igneous provinces (LIPs), episodes of sustained and voluminous volcanic activity, are thought to drive global climatic change. However, the balance between the warming (via CO_2 emission) and cooling (via enhanced weathering) impacts of LIPs is poorly understood. Here we use a modelling approach which considers both warming and cooling as a result of LIP emplacement for the period 300 – 150 million years ago (during the breakup of the supercontinent Pangea). We show that only the Central Atlantic Magmatic Province leads to cooling in our model, with no significant temperature reduction for any other LIPs. This implies that LIPs and basaltic material do not driver of global cooling on multimillion year timescales via enhanced weathering.

Main Text

The emplacement of large igneous provinces (LIPs), systems of voluminous mafic magmatism (more than 10^6 km^3 volcanic material), related to processes other than seafloor spreading has occurred regularly through Earth's history (1–3). The release of enormous quantities of greenhouse gases, and the emplacement of considerable volcanic terranes associated with LIPs are known to impact many global biogeochemical cycles (2, 4, 5). As a result, linkages between LIP emplacement and large-scale changes in the Earth system, and especially environmental and climatic shifts, are often made (2, 6, 7), convincingly linking LIP emplacement to a number of mass extinctions (1, 2, 8–10). In addition to their potential importance in geologically rapid perturbations of the Earth system such as those observed during mass extinctions, LIPs may be important for setting the climate state of Earth over longer time periods (11), potentially as drivers of long-term cooling (11, 12).

The period between 300 and 150 million years ago (Ma), when the supercontinent Pangaea began to rift and break apart, initiated many of the Earth system and evolutionary upheavals that led to the planet's current configuration. During this time some of the largest LIPs in Earth history were emplaced, sometimes coinciding with mass extinctions. These include the Siberian Traps (252 Ma), which is the largest continental LIP by volume, and widely thought to be the driver of the End-Permian Mass Extinction(13–16). Later in the Mesozoic, the Central Atlantic Magmatic Province (CAMP; 201 Ma), the largest continental LIP by area, has been linked to the end-Triassic extinction(17–19). Further, the Karoo and Ferrar LIPs (183 Ma) have been implicated in the end-Pliensbachian extinction, and Toarcian anoxic event(20–22) respectively.

It is generally assumed that the primary kill mechanism of LIPs is carbon-rich volatile release (especially CO, CO_2 and CH_4) enhancing the greenhouse effect and resulting in catastrophic global warming(2, 8, 9, 23). This is especially true for rare examples of LIPs that were emplaced into organic carbon-rich sediment, such as the Siberian Traps (16, 24). However, research has also shown how large volcanic episodes can lead to long-term global cooling (12, 17, 25). This cooling can occur via the supply of mantle- or crustal-derived nutrients to the oceans leading to enhanced carbon sequestration via the biological pump (25, 26), and through an enhanced silicate weathering cycle fueled by highly weatherable volcanic rocks (4, 17, 27). Consequently, the holistic impact of LIP emplacement on climate is uncertain, and very few modelling studies consider concurrently the likely cooling and warming impact of LIPs together (11, 27), with no studies we know of prior to the Deccan Traps (66 Ma). As such, the exact balance between cooling and warming is unclear (28).

To determine if Mesozoic LIPs could have led to cooling on multimillion year timescales, and to investigate the cumulative impact of numerous LIP emplacements, we use a long-term climate-biogeochemical model (*SCION* (27, 29)) integrated with the record of LIP emplacement between 300 and 150 Ma (30). As well as incorporating volumes of degassed CO_2 during emplacement, these LIPs are added to the 2D model land surface grid as basaltic terranes and interact with local temperature, relief and hydrology to amplify silicate weathering rates (Fig. 1). Our approach therefore allows us to simultaneously consider the warming and cooling potential of each individual LIP on the Earth system over long timescales through this period of climatic and evolutionary upheaval to present a holistic view of LIP emplacement.

Results and Discussion

The role of LIPs in cooling the Mesozoic Earth system

The inclusion of LIPs in the *SCION* model clearly alters the model reconstruction of climate between 300–150 Ma (Figs. 2, 3). By calculating a total carbon balance between the input of carbon from a LIP minus the removal of carbon via LIP weathering (see Methods), we can disentangle the overall impact of individual LIPs on the Earth system on multimillion year timescales.

Our model results identify that on multimillion year timescales, LIP weathering is the dominant driver of LIP-related carbon cycling perturbations, with the majority of the studied time frame characterised by LIP-induced carbon drawdown (Fig. 2). This makes sense as LIPs become a permanent feature of the weathering environment, whereas CO_2 release is short-lived. The suggestion that LIPs may lead to global cooling has been made previously (11, 12, 31, 32), but it has been so far challenging to quantify the exact balance between LIP carbon emission and removal (28).

At 300 Ma LIPs are a net CO_2 sink in the model, reflecting the weathering of previously-established terranes. Following the Siberian Traps (252 Ma) emplacement is slight enhancement of net LIP-related

CO_2 drawdown in the model (Fig. 2), reflecting the weathering of Siberian Trap material (33), but the location of this LIP in the high latitudes means the silicate weathering feedback is much weaker than if it were emplaced in the tropics (32). The signature of this weathering is also noticeable in the seawater $^{87}Sr/^{86}Sr$, which in the weathering-only scenario, declines slightly in the period following the emplacement of the Siberian Traps (Fig. 4). From 220 Ma onwards, global cooling, driven by pCO_2 reduction in the period 220–200 Ma is reconstructed by SCION, but was a feature of the original model so is not related to LIP activity.

The CAMP, emplaced from 200 Ma onwards in the model, leads to the highest LIP-related carbon burial values in the Mesozoic (Fig. 2). The location of the CAMP across the equatorial region (Figs 1, 2) and adjacent to an incipient ocean basin, means it is subjected to the most intense chemical weathering regime (29). The impact of this weathering is most clearly seen in the model seawater $^{87}Sr/^{86}Sr$ record, which diverges considerably from the baseline *SCION* run and is much closer to proxy reconstructions (Fig. 4). Intense weathering leads to effective CO_2 drawdown through silicate weathering and carbonate deposition, and also through nutrient delivery to oceans coupled with a strong biological pump, resulting in high levels of organic carbon burial in the model. The action of both these carbon sinks leads to slightly cooler climate between 200–180 Ma relative to baseline *SCION* (Fig. 4), but it is noticeable that this shift is only around 1°C (Figs. 3,4), echoed by a small decrease in pCO_2. This shift may go a small way to reconciling the early Jurassic cooling, an event which has proven enigmatic to explain (34, 35). However, cooling of up to 5°C, as seen in some proxy records in the early Jurassic (34) is not reproduced by our model. It is possible that we underestimate the level of weatherability enhancement represented by basaltic LIP emplacement, meaning we underestimate the cooling impact of LIPs. However, the good correspondence between the seawater $^{87}Sr/^{86}Sr$ record and our model results suggests the amount of additional unradiogenic material being input to the oceans is of the correct order of magnitude (Fig. 3). A weathering enhancement value of seven-fold, as used by previous studies(11, 27), therefore appears suitable, suggesting LIPs—even the massive CAMP—are unable to cause considerable cooling on multimillion year timescales. From 200–150 Ma, the ongoing influence of CAMP basalt weathering is evident in the modelled outputs, keeping global temperatures and pCO_2 low despite the emplacement and degassing of two other major LIPs. These LIPs (the Karoo-Ferrar and the NW Australian) have only short-term impacts on temperatures and *p*CO2 (Fig. 4).

One of the clearest impacts of the addition of LIPs to the *SCION* model is on the Sr isotope system. Prior to LIP addition, the model is unable to reproduce most of the Mesozoic trends in oceanic Sr isotope composition (Fig. 4). This offset has previously been linked to the poor availability of surface lithological data(29, 36), and so the inclusion of a LIPs as sources of Sr with igneous signatures more strongly reconciles model outputs with the geological record. In particular, the long-term drop in seawater $^{87}Sr/^{86}Sr$ after 200 Ma, after the CAMP emplacement, is well produced by our updated *SCION* model, and is linked to enhanced basaltic weathering from the emplacement of the LIP at this time (Fig. 4), where this basalt has a mantle-like Sr isotope composition and therefore acts to reduce seawater $^{87}Sr/^{86}Sr$. Further, the addition of Sr input from temperature-induced continental weathering also improves the comparability of the data to the model outputs, particularly across the P–T boundary, where $^{87}Sr/^{86}Sr$ rises markedly, a rise driven by the global warming impact of the Siberian Traps and weathering of generally radiogenic crustal material – as the LIP was emplaced away from major weathering zones.

Outside of the Siberian Traps and the CAMP, for most of the time between 300–150 Ma, there is little evidence of LIPs driving large scale, multimillion year cooling through enhanced weathering in our model, countering suggestions that LIP weathering is a long-term driver of cool climate(37, 38). Our finding here agrees with work which finds no correlation between LIP area and ice sheet size(30), and suggests that any correspondence between emplacement and long-term cooling may not be LIP-weathering related. It is possible the deposition of volcanic ash, known to drive periods of transient cooling (12), may be more important than basalt emplacement as a driver of CO_2 removal (26) on long time scales.

LIPs and warming in the Mesozoic

Despite our focus on the cooling impact of LIPs, to consider their holistic impact we also model carbon degassing. Our model reconstructs degassing rates using the timing of LIP emplacement unless the exact period of degassing is known (see Methods). As such, if degassing occurred over extremely short timescales such as centuries, as proposed for the CAMP(39), our model would not capture this short-term warming.

As expected, we see transient warming events during the largest LIP emplacements in our study period (Figs. 2,4). At the end of the Permian and beginning of the Jurassic periods, the impact of massive, rapid carbon release from LIPs is clear (Fig. 4). Compared to other LIPs in the Mesozoic, the speed and scale of carbon release during the emplacement of the Siberian Traps is nearly an order of magnitude higher (Fig. 3). In baseline *SCION* runs, transient carbon cycle perturbations from LIPs are not included (Fig. 3, red line), but in the new model scenario, the P–T boundary is represented by a shift to pCO_2 as high as 10,000 ppm, reflective of proxy data from the period (15). This is reflected in the modelled Global Average Temperature (GAT), which rises roughly 7°C across the P–T. However, this rise is well below what has been reconstructed using proxy data, which shows up to 15°C rise in tropical temperatures (and thus persumably more at the global scale) across the P–T(40, 41). This disconnect is potentially related to the low climate sensitivity and relatively high pre-event CO_2 within *SCION*. Later in the Mesozoic, we also see the warming impact of the emplacement of the Central Atlantic Magmatic Province (201 Ma), with a rise of 4°C in our model (Fig. 4). This contrasts with reconstructions of above 5°C change (42) or up to 16°C change in some proxy data (43). For the Karoo-Ferrar (182 Ma), we see a rise of 3°C. Again, this is below proxy reconstructions of between 4 - 7°C shift across this interval (44, 45).

Our results for LIP warming tend to be less extreme than previous proposals. This may be because our degassing rates are controlled by the length of LIP emplacement, and so may result in underestimation of rates if pulsed degassing during the LIP occurred. By running comparative models which reduce the degassing window to 50 ka for each event, we can reconstruct changes in climate which are much closer to proxy reconstructions (Fig. 4, dashed cyan line). In this scenario, the temperature rise across the P-T is 12°C, and for the CAMP it is 8°C, much closer to previous reconstructions (Fig. 4).

Implications

Most studies linking LIPs to global climatic change have focussed on the warming impact of LIPs. Conversely, other studies purport that weathering of highly reactive basaltic terranes associated with LIP emplacement is a driver of global cooling (17, 37, 38, 46). However, while we reconstruct the short-term warming in our model, we see little evidence of most Mesozoic LIPs having a cooling impact. The one exception here is the emplacement of the CAMP, which drives global cooling (>1°C) associated with enhanced organic carbon and carbonate burial and $p\mathrm{CO_2}$ reduction. The correspondence of our modelled seawater $^{87}\mathrm{Sr}/^{86}\mathrm{Sr}$ and proxy records suggests the model weatherability parameters are suitable and that the input of weathered material as simulated in our model is on the correct order of magnitude. We conclude, therefore, that LIPs do not have a major cooling impact on the Earth's climate, except when a spatially extensive LIP is emplaced in the tropics such as the CAMP. However, even with extensive tropical LIP emplacement, our model suggests it is unlikely that LIPs can drive global glaciations (Fig. 4), as has been suggested (46).

As discussed, the link between LIPs and glaciation and/or climate cooling has been made in numerous previous studies, but these studies are correlative, and so testing of the feasibility of a causative link has not been completed (46). Our work suggests it is unlikely the Tarim, Panjal, Emeishan or Choiyoi LIPs had any driving roles in the successive glacial periods of the early Permian (the so-called P1-P4 events (47)), as has been suggested (25, 48). We also consider it unlikely that the Karoo-Ferrar LIP drove the late Pleinsbachian cooling and the Jurassic icehouse episodes (46, 49). Indeed, it is telling that the emplacement of the one LIP able to drive global cooling in our model, the CAMP, is not implicated in any global cooling events (30, 46, 50).

Our findings may also have implications for other periods of Earth's history such as the Cenozoic, where weathering of basaltic material has been implicated in the cooling trend after the Eocene (51). Recent work has suggested the Afro-Arabian LIP may be a source of weatherable material in the early Oligocene (46), but our modelling suggests that the size and location of the LIP (a relatively small LIP emplaced in an arid area) mean the impact on global climate is likely to be negligible. Looking further back in time, the emplacement of the Franklin LIP has been suggested as a driver of runaway cooling and eventual Snowball Earth development around 720 Ma (52, 53). However, again our work appears to suggest a causative link is unlikely, even if the Franklin LIP was emplaced as a high-relief terrane in the humid, tropical Neoproterozoic (52).

As demonstrated by this study, the location of the LIP material is key to determining the importance of its weathering in global biogeochemistry. As a result, accurate plate reconstructions are vital, as the LIP placement is reliant upon them. In particular, paleolatitude is central to the determination of a LIP's location within or outside of a tropical or mid-latitude rain belt (30). Therefore, to determine exactly how LIPs drive cooling, work must be completed to improve plate reconstructions in deeper time and coupled to improved reconstruction of exact extent and location of LIPs.

Methods

We use the *SCION* (Spatial Continuous Integration) Earth Evolution model version 1.1 in this work but with a number of additions as outlined below. SCION combines a long-term biogeochemical box model with a 3D interpolated steady state climate and a 2D continental lithology and weathering module. We run the simulation forwards for the whole Phanerozoic, but only display the output of the period 300–150 Ma as we intend to focus on the impact of the largest LIPs in Earth history in detail, rather than a general investigation of the entire Phanerozoic. For ease of comprehension, we focus on the outputs of atmospheric CO_2, global average temperature, whole ocean $\delta^{13}C$ and $^{87}Sr/^{88}Sr$. Model code is included in the submission, and will be made available on Github if the manuscript is accepted.

Addition of Large Igneous Provinces as highly weatherable terranes

As in previous work (27), we include LIPs as weatherable terranes in the SCION GCM interpolation stacks (see Supplementary Table 1). For this work, we mapped the locations of each LIP onto the palaeogeographic land-sea masks of the SCION model (Fig. 1). We used the compilation of ref.(30), which is based on two prior compilations (2, 6).

In the study of ref.(30), the authors reconstruct the original, full extent of LIPs when and where they were emplaced as a series of digital polygons. They then determine a statistical relationship using the present-day arial extent of LIPs and age (i.e. time since emplacement) and found an exponential relationship between the data. Ref.(30) calculated a LIP half-life of 29 Ma (increasing to 36 Ma if one accounts for burial of LIPs—which we do not use in our analysis) (Equations 1 and 2), allowing us to calculate a fractional area of each LIP at a time after it's emplacement (A_{decay}):

$$A_{decay} = A\, e^{-\lambda \bullet t} \text{ (Equation 1)}$$

$$\lambda = \frac{log(2)}{T_{1/2}} \text{ (Equation 2)}$$

With A being original areal content (=1); λ, the decay constant; t, time since emplacement, and; $T_{1/2}$, the calculated half-life (=29 Ma). Therefore, at each GCM data-stack timeslice we rasterize the LIP polygons from ref.(30) onto a 40•48 grid (which is the resolution of the underlying FOAM GCM in *SCION*) at their correct location. This gives us a grid of '0s' and '1s' representing cells of either non-LIP or LIP respectively. We then calculate the fractional content of each LIP cell that has eroded according to Equation 1 after ref.(30) and update the relevant cell to reflect this (so after emplacement LIP cells will be between 0 and 1). Finally, because the palaeogeographic model used in the *SCION* model is slightly different to that used by ref.(30), some manual manipulation of the gridcells was required to ensure they were placed correctly with respect to the palaeogeography. We complete this exercise for each individual LIP, so for the Mesozoic, we have 7 individual LIP maps which vary through time. SCION uses a 'double keyframing' approach to calculate continental processes in between the GCM climate simulation times. For example, at 20 Ma the model is looking at both the 30Ma and 15Ma GCM simulations and averaging between then. As most LIPs are emplaced between the keyframe times, we include a 'switch-on' in the code. This checks the time of emplacement for each LIP, and when the model has reached that point, the LIP appears as a weatherable terrane in both the previous and next GCM paleogeography. See Supplementary Text for further information on the LIP digitization approach.

The model considers all land other than LIPs to be a homogenous mixture (29), which is calculated to be 7 times less weatherable for silicates than LIP basalts. This estimate is based on previous research indicating the weatherability of mafic rocks to be around seven times greater than that of silicates (54), and is the same factor as used in previous work (27, 32). As we are adding large areas of weatherable material to the model, we remove the original global basalt weathering curve outlined in ref (29). As such, we assume that LIPs represent most of the total basalt emplaced through the period.

Addition of LIP degassing

As with previous work, we also consider the potential for LIP emplacement to release significant quantities of CO_2 and CH_4 into the atmosphere (27). To estimate the amount of carbon emitted from each LIP, we use two primary approaches. For those LIPs which are well studied and for which degassing rates or total carbon emission estimates have been made (e.g. Siberian Traps; ref.(14)), we take published flux values or calculate them using the timeframe of LIP emplacement and total carbon release. For those LIPs which are not as well understood, we use published estimates of the volume (in km^3) of magma emplaced and the duration of the LIP (in kyrs) to produce an estimate of magma emplacement in km^3/kyr. We then convert this value to an estimate of carbon degassing using a conversion factor. For silicic LIPs, we use the same approach as ref.(25), which calculates an emission rate of 10^{11} g C per km^3 of magma emplacement, based upon an estimate of 500 ppm CO_2 in the pre-eruptive magma (55). For basaltic LIPs, we assume pre-eruptive CO_2 content of 0.5 wt%, and so an emission rate of 10^{12} g C per km^3. For modelling purposes, these values are converted to molar carbon flux. For each LIP, the rate estimate is used to emit CO_2 into the model atmosphere. We use Gaussian curves to complete this, with the midpoint of the LIP activity and the peak of carbon emissions used to construct the function (see Supplementary Table 1). We set the width of the Gaussian function to be related to the period of activity known for the LIP. For example, the Siberian Traps is taken to have degassed in 1 Myr (56), and the Karoo in 0.47 Myrs (57), see Supplementary Table 1 for all LIP details. To test the impact of shorter function length on degassing rates and global climate, we also run the model with a set of fixed Gaussian widths for all LIPs. For this exercise, we set all LIP degassing functions to 0.05 Ma (Fig. 1). For carbon isotopic mass balance, we include a new 'LIP CO_2 $\delta^{13}C$' estimate in the model, which we take to be -5 ‰, and is the isotopic composition of the degassed CO_2.

Model scenarios

The aim of this work is to investigate the holistic role of LIP emplacement on the Earth system. However, we also test the dependence of the model upon each individual factor associated with LIP emplacement. For this, we construct a number of model scenarios. The first, which we term 'Baseline' is SCION version 1.1 without any model additions. Second is the preferred model, which we term 'Weathering & Degassing', which includes both the impact of weatherable LIPs and their carbon degassing. A further model considers the system with only degassing and no enhanced weatherability (LIP weatherability set to the same as homogeneous silicates), termed 'Degassing Only'. Our final model scenario considers the system with no carbon degassing, but with the enhanced weatherability of LIPs included, and is termed 'Weathering Only'. For the 'Weathering & Degassing' scenario we perform sensitivity tests, completed via the running of 1000 simulations with random variation of a number of variables following previous work (27, 29). Results of the sensitivity analysis can be found in Supplementary Figure 2.

Carbon Balance Calculations

We use the mean values of the 'Weathering & Degassing' scenario to calculate an overall carbon balance. That is the total impact of LIP emplacement on carbon cycling. For this we subtract C associated with basalt weathering (*basw* in the model) from the LIP degassing rate (*LIP_CO2* in the model outputs), resulting in a value of carbon perturbation associated with LIP emplacement at each time step (Fig. 1a).

Acknowledgements

B.J.W.M. and A.S.M. acknowledge funding from UKRI grant NE/X011208/1.

Author Contributions

J.L. and B.J.W.M. conceived the research. J.L. and A.S.M. amended the SCION code for this work. J.L. completed the modelling and made the figures. J.L. wrote the original manuscript, with input from B.J.W.M. and A.S.M.

Competing Interests

The authors declare no competing interests.

Data access

There is no original data associated with this publication.

Code access

SCION model code is available at https://github.com/bjwmills/SCION. The code version used in this manuscript is submitted alongside this manuscript and will be uploaded to Github if the manuscript is accepted.

Rights

References

1. S. V. Sobolev, *et al.*, Linking mantle plumes, large igneous provinces and environmental catastrophes. *Nature* **477**, 312–316 (2011).

2. R. E. Ernst, N. Youbi, How Large Igneous Provinces affect global climate, sometimes cause mass extinctions, and represent natural markers in the geological record. *Palaeogeogr Palaeoclimatol Palaeoecol* **478**, 30–52 (2017).

3. B. A. Black, L. Karlstrom, T. A. Mather, The life cycle of large igneous provinces. *Nature Reviews Earth & Environment 2021 2:12* **2**, 840–857 (2021).

4. M. T. Jones, D. A. Jerram, H. H. Svensen, C. Grove, The effects of large igneous provinces on the global carbon and sulphur cycles. *Palaeogeogr Palaeoclimatol Palaeoecol* **441**, 4–21 (2016).

5. B. A. Black, S. A. Gibson, Deep Carbon and the Life Cycle of Large Igneous Provinces. *Elements* **15**, 319–324 (2019).

6. R. E. Ernst, *et al.*, "Large Igneous Province Record Through Time and Implications for Secular Environmental Changes and Geological Time-Scale Boundaries" in *Large Igneous Provinces: A Driver of Global Environmental and Biotic Changes*, (2021), pp. 1–26.

7. J. P. Pu, *et al.*, Emplacement of the Franklin large igneous province and initiation of the Sturtian Snowball Earth. *Sci Adv* **8** (2022).

8. D. P. G. Bond, S. E. Grasby, On the causes of mass extinctions. *Palaeogeogr Palaeoclimatol Palaeoecol* **478**, 3–29 (2017).

9. P. B. Wignall, Large igneous provinces and mass extinctions. *Earth Sci Rev* **53**, 1–33 (2001).

10. T. Green, P. R. Renne, C. B. Keller, Continental flood basalts drive Phanerozoic extinctions. *Proceedings of the National Academy of Sciences* **119**, e2120441119 (2022).

11. V. Lefebvre, Y. Donnadieu, Y. Goddéris, F. Fluteau, L. Hubert-Théou, Was the Antarctic glaciation delayed by a high degassing rate during the early Cenozoic? *Earth Planet Sci Lett* **371–372**, 203–211 (2013).

12. J. Longman, B. J. W. Mills, H. R. Manners, T. M. Gernon, M. R. Palmer, Late Ordovician climate change and extinctions driven by elevated volcanic nutrient supply. *Nat Geosci* **14**, 924–929 (2021).

13. B. A. Black, *et al.*, Systemic swings in end-Permian climate from Siberian Traps carbon and sulfur outgassing. *Nat Geosci* **11**, 949–954 (2018).

14. J. Dal Corso, *et al.*, Permo–Triassic boundary carbon and mercury cycling linked to terrestrial ecosystem collapse. *Nat Commun* **11**, 1–9 (2020).

15. Y. Wu, *et al.*, Six-fold increase of atmospheric pCO2 during the Permian–Triassic mass extinction. *Nature Communications 2021 12:1* **12**, 1–8 (2021).

16. H. Svensen, *et al.*, Siberian gas venting and the end-Permian environmental crisis. *Earth Planet Sci Lett* **277**, 490–500 (2009).

17. M. F. Schaller, J. D. Wright, D. V. Kent, P. E. Olsen, Rapid emplacement of the Central Atlantic Magmatic Province as a net sink for CO2. *Earth Planet Sci Lett* **323–324**, 27–39 (2012).

18. M. Capriolo, *et al.*, Anthropogenic-scale CO2 degassing from the Central Atlantic Magmatic Province as a driver of the end-Triassic mass extinction. *Glob Planet Change* **209**, 103731 (2022).

19. T. J. Blackburn, *et al.*, Zircon U-Pb geochronology links the end-triassic extinction with the central Atlantic magmatic province. *Science (1979)* **340**, 941–945 (2013).

20. T. Müller, *et al.*, Ocean acidification during the early Toarcian extinction event: Evidence from boron isotopes in brachiopods. *Geology* **48**, 1184–1188 (2020).

21. L. M. E. Percival, *et al.*, Globally enhanced mercury deposition during the end-Pliensbachian extinction and Toarcian OAE: A link to the Karoo–Ferrar Large Igneous Province. *Earth Planet Sci Lett* **428**, 267–280 (2015).

22. A. H. Caruthers, P. L. Smith, D. R. Gröcke, The Pliensbachian–Toarcian (Early Jurassic) extinction, a global multi-phased event. *Palaeogeogr Palaeoclimatol Palaeoecol* **386**, 104–118 (2013).

23. M. F. Schaller, J. D. Wright, D. V. Kent, Atmospheric PCO2 perturbations associated with the central atlantic magmatic province. *Science (1979)* **331**, 1404–1409 (2011).

24. C. Ganino, N. T. Arndt, Climate changes caused by degassing of sediments during the emplacement of large igneous provinces. *Geology* **37**, 323–326 (2009).

25. S. M. Cather, N. W. Dunbar, F. W. McDowell, W. C. McIntosh, P. A. Scholle, Climate forcing by iron fertilization from repeated ignimbrite eruptions: The icehouse-silicic large igneous province (SLIP) hypothesis. *Geosphere* **5**, 315–324 (2009).

26. J. Longman, M. R. Palmer, T. M. Gernon, H. R. Manners, The role of tephra in enhancing organic carbon preservation in marine sediments. *Earth Sci Rev* **192**, 480–490 (2019).

27. J. Longman, B. J. W. Mills, Y. Donnadieu, Y. Goddéris, Assessing Volcanic Controls on Miocene Climate Change. *Geophys Res Lett* **49** (2022).

28. C.-T. Lee, S. Dee, Does volcanism cause warming or cooling? *Geology* **47**, 687–688 (2019).

29. B. J. W. Mills, Y. Donnadieu, Y. Goddéris, Spatial continuous integration of Phanerozoic global biogeochemistry and climate. *Gondwana Research* (2021). https://doi.org/10.1016/j.gr.2021.02.011.

30. Y. Park, N. L. Swanson-Hysell, L. E. Lisiecki, F. A. Macdonald, Evaluating the Relationship Between the Area and Latitude of Large Igneous Provinces and Earth's Long-Term Climate State. *Large Igneous Provinces: A Driver of Global Environmental and Biotic Changes* 153–168 (2021). https://doi.org/10.1002/9781119507444.CH7.

31. F. A. Macdonald, N. L. Swanson-Hysell, Y. Park, L. Lisiecki, O. Jagoutz, Arc-continent collisions in the tropics set Earth's climate state. *Science (1979)* **364**, 181–184 (2019).

32. Y. Goddéris, *et al.*, Onset and ending of the late Palaeozoic ice age triggered by tectonically paced rock weathering. *Nat Geosci* **10**, 382–386 (2017).

33. X. Y. Chen, F. Z. Teng, K. J. Huang, T. J. Algeo, Intensified chemical weathering during Early Triassic revealed by magnesium isotopes. *Geochim Cosmochim Acta* **287**, 263–276 (2020).

34. G. Dera, *et al.*, Climatic ups and downs in a disturbed Jurassic world. *Geology* **39**, 215–218 (2011).

35. S. D. Schoepfer, T. J. Algeo, B. van de Schootbrugge, J. H. Whiteside, The Triassic–Jurassic transition – A review of environmental change at the dawn of modern life. *Earth Sci Rev* **232**, 104099 (2022).

36. B. Mills, S. J. Daines, T. M. Lenton, Changing tectonic controls on the long-term carbon cycle from Mesozoic to present. *Geochemistry, Geophysics, Geosystems* **15**, 4866–4884 (2014).

37. Z. Gong, M. Zhang, J. Li, C. Huang, Late Permian ∼ 6 My cooling induced by basaltic weathering of the Emeishan large igneous province: Evidence from interbasaltic paleosols. *Palaeogeogr Palaeoclimatol Palaeoecol* **609**, 111305 (2023).

38. J. Yang, *et al.*, Enhanced continental weathering and large igneous province induced climate warming at the Permo-Carboniferous transition. *Earth Planet Sci Lett* **534**, 116074 (2020).

39. M. Capriolo, *et al.*, Deep CO2 in the end-Triassic Central Atlantic Magmatic Province. *Nature Communications 2020 11:1* **11**, 1–11 (2020).

40. Y. Sun, *et al.*, Lethally hot temperatures during the early triassic greenhouse. *Science (1979)* **338**, 366–370 (2012).

41. C. R. Scotese, H. Song, B. J. W. Mills, D. G. van der Meer, Phanerozoic paleotemperatures: The earth's changing climate during the last 540 million years. *Earth Sci Rev* [Preprint] (2021). [Accessed 3 May 2021].

42. T. T. Huynh, C. J. Poulsen, Rising atmospheric CO2 as a possible trigger for the end-Triassic mass extinction. *Palaeogeogr Palaeoclimatol Palaeoecol* **217**, 223–242 (2005).

43. V. A. Petryshyn, *et al.*, The role of temperature in the initiation of the end-Triassic mass extinction. *Earth Sci Rev* **208**, 103266 (2020).

44. G. Suan, E. Mattioli, B. Pittet, S. Mailliot, C. Lécuyer, Evidence for major environmental perturbation prior to and during the Toarcian (Early Jurassic) oceanic anoxic event from the Lusitanian Basin, Portugal. *Paleoceanography* **23** (2008).

45. T. R. Bailey, Y. Rosenthal, J. M. McArthur, B. van de Schootbrugge, M. F. Thirlwall, Paleoceanographic changes of the Late Pliensbachian–Early Toarcian interval: a possible link to the genesis of an Oceanic Anoxic Event. *Earth Planet Sci Lett* **212**, 307–320 (2003).

46. N. Youbi, *et al.*, “Preliminary Appraisal of a Correlation Between Glaciations and Large Igneous Provinces Over the Past 720 Million Years” in (2021), pp. 169–190.

47. J. G. Ogg, G. M. Ogg, F. M. Gradstein, *A Concise Geologic Time Scale* (Elsevier, 2016).

48. J. L. Isbell, P. A. Lenaker, R. A. Askin, M. F. Miller, L. E. Babcock, Reevaluation of the timing and extent of late Paleozoic glaciation in Gondwana: Role of the Transantarctic Mountains. *Geology* **31**, 977 (2003).

49. C. Korte, *et al.*, Jurassic climate mode governed by ocean gateway. *Nat Commun* **6**, 10015 (2015).

50. A. Marzoli, *et al.*, “The Central Atlantic Magmatic Province (CAMP): A Review” in (2018), pp. 91–125.

51. D. V. Kent, G. Muttoni, Modulation of Late Cretaceous and Cenozoic climate by variable drawdown of atmospheric <i>p</i>CO₂ from weathering of basaltic provinces on continents drifting through the equatorial humid belt. *Climate of the Past* **9**, 525–546 (2013).

52. F. Dufour, *et al.*, New U-Pb CA-ID TIMS zircon ages implicate the Franklin LIP as the proximal trigger for the Sturtian Snowball Earth event. *Earth Planet Sci Lett* **618**, 118259 (2023).

53. J. P. Pu, *et al.*, Emplacement of the Franklin large igneous province and initiation of the Sturtian Snowball Earth. *Sci Adv* **8** (2022).

54. C. Dessert, B. Dupré, J. Gaillardet, L. M. François, C. J. Allègre, Basalt weathering laws and the impact of basalt weathering on the global carbon cycle. *Chem Geol* **202**, 257–273 (2003).

55. Y. Liu, A. T. Anderson, C. J. N. Wilson, A. M. Davis, I. M. Steele, Mixing and differentiation in the Oruanui rhyolitic magma, Taupo, New Zealand: evidence from volatiles and trace elements in melt inclusions. *Contributions to Mineralogy and Petrology* **151**, 71–87 (2006).

56. S. D. Burgess, S. A. Bowring, High-precision geochronology confirms voluminous magmatism before, during, and after Earth's most severe extinction. *Sci Adv* **1** (2015).

57. H. Svensen, F. Corfu, S. Polteau, Ø. Hammer, S. Planke, Rapid magma emplacement in the Karoo Large Igneous Province. *Earth Planet Sci Lett* **325–326**, 1–9 (2012).

Figures

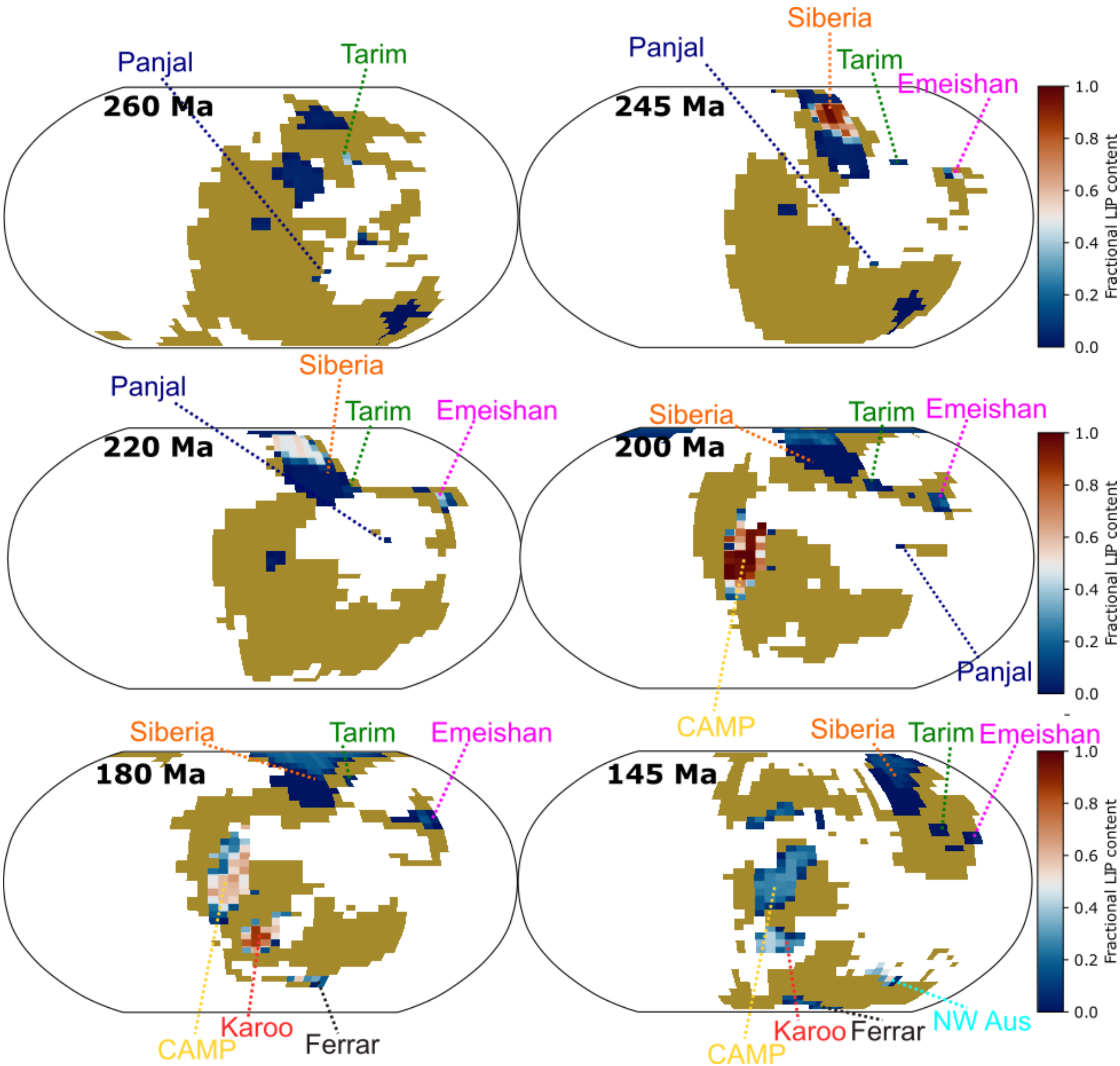

Figure 1 | Location of Large Igneous Provinces (LIPs) considered in this study. Each panel demonstrates the location of each LIP at each time point. Ocean is coloured white whilst mustard is used to highlight the land cover on each map. Overlain are LIP locations which are coloured by their fractional cover, from blue (very low LIP cover) to red (complete LIP cover). These fractional values are used to calculate weathering fluxes for each grid square (see Methods).

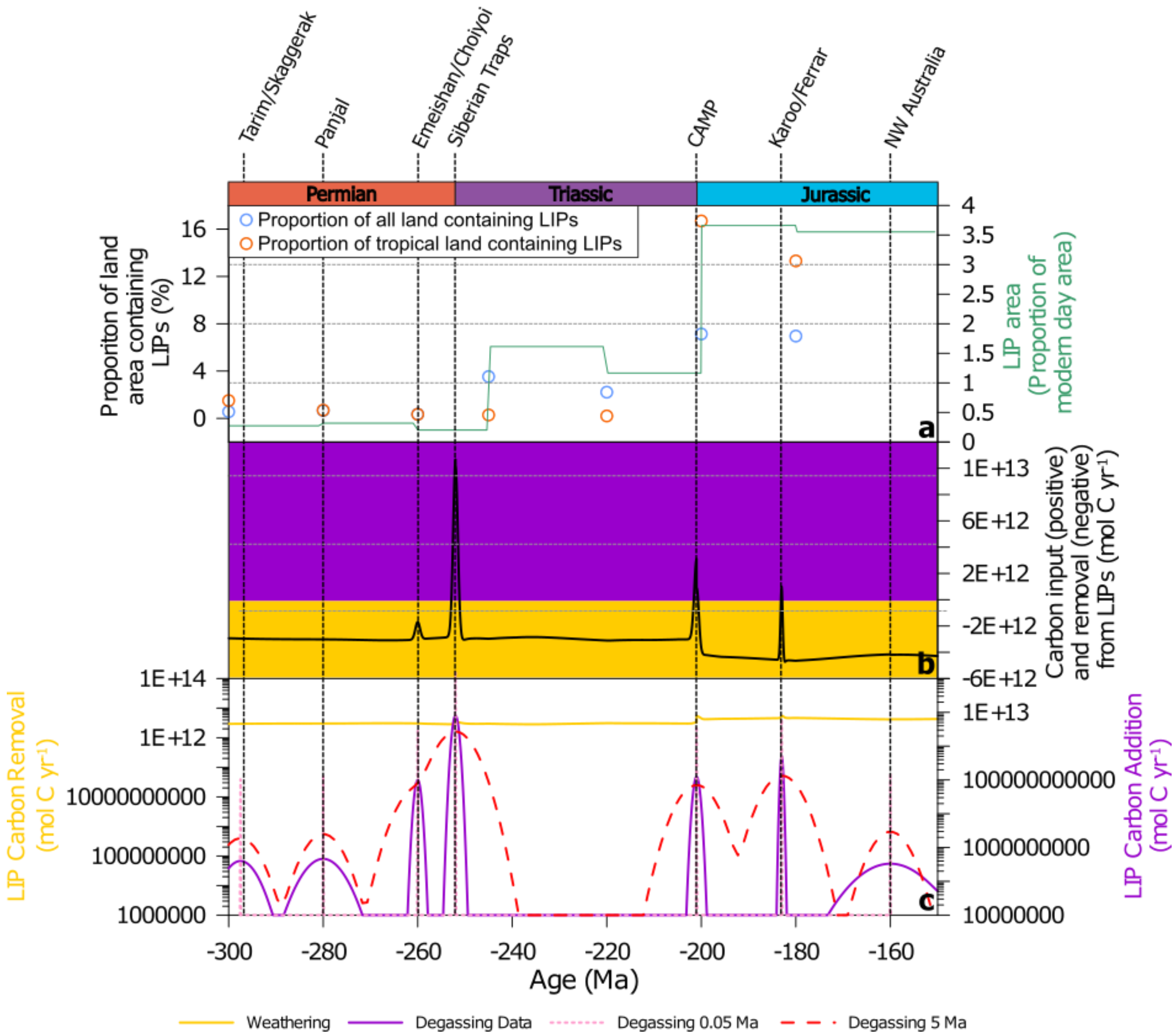

Figure 2 | Carbon cycle forcing as a result of Large Igneous Province (LIP) emplacement. (a) The percentage of terrestrial grid squares in each GCM run to contain some LIP material (blue circles) and the percentage of these squares in the tropics which contain LIP material (orange circles). Plotted alongside relative LIP area versus present (green) (b) Overall carbon balance as a result of LIP input and removal of carbon from the Earth system (see Methods). (c) Components of the overall LIP carbon balance, with LIP degassing in purple and carbon burial via enhanced silicate weathering in yellow.

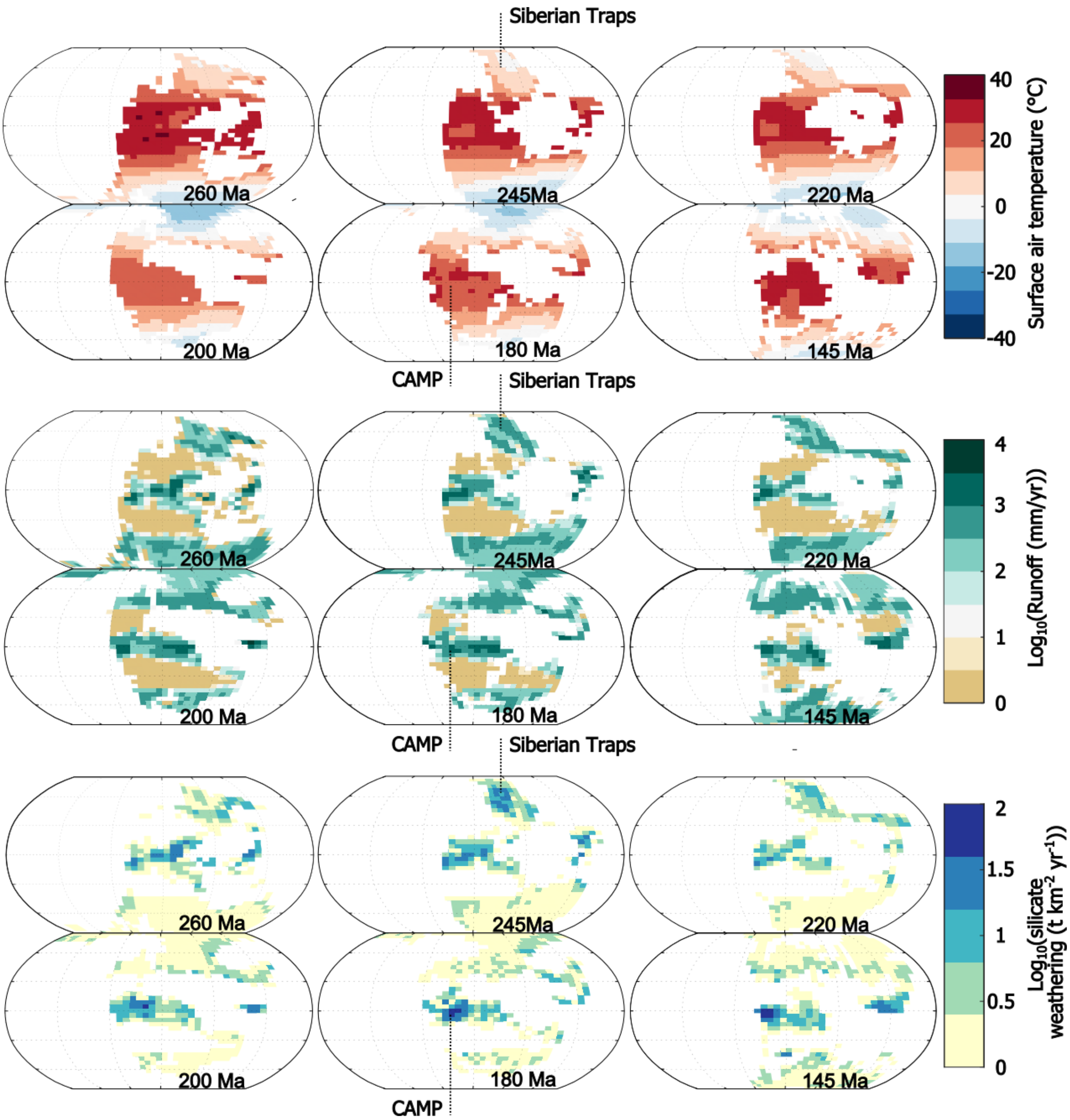

Figure 3 | Gridded map outputs for the 'Weathering & Degassing' scenario across the period 300 – 150 Ma. In the upper panel surface air temperature is displayed, with continental runoff in the middle panel silicate weathering fluxes in the bottom panel. In each map, intensity of the variable from each grid square is indicated via colour bar. The location of the two largest LIPs of the Mesozoic (the Siberian Traps and the Central Atlantic Igneous Province) are specifically highlighted.

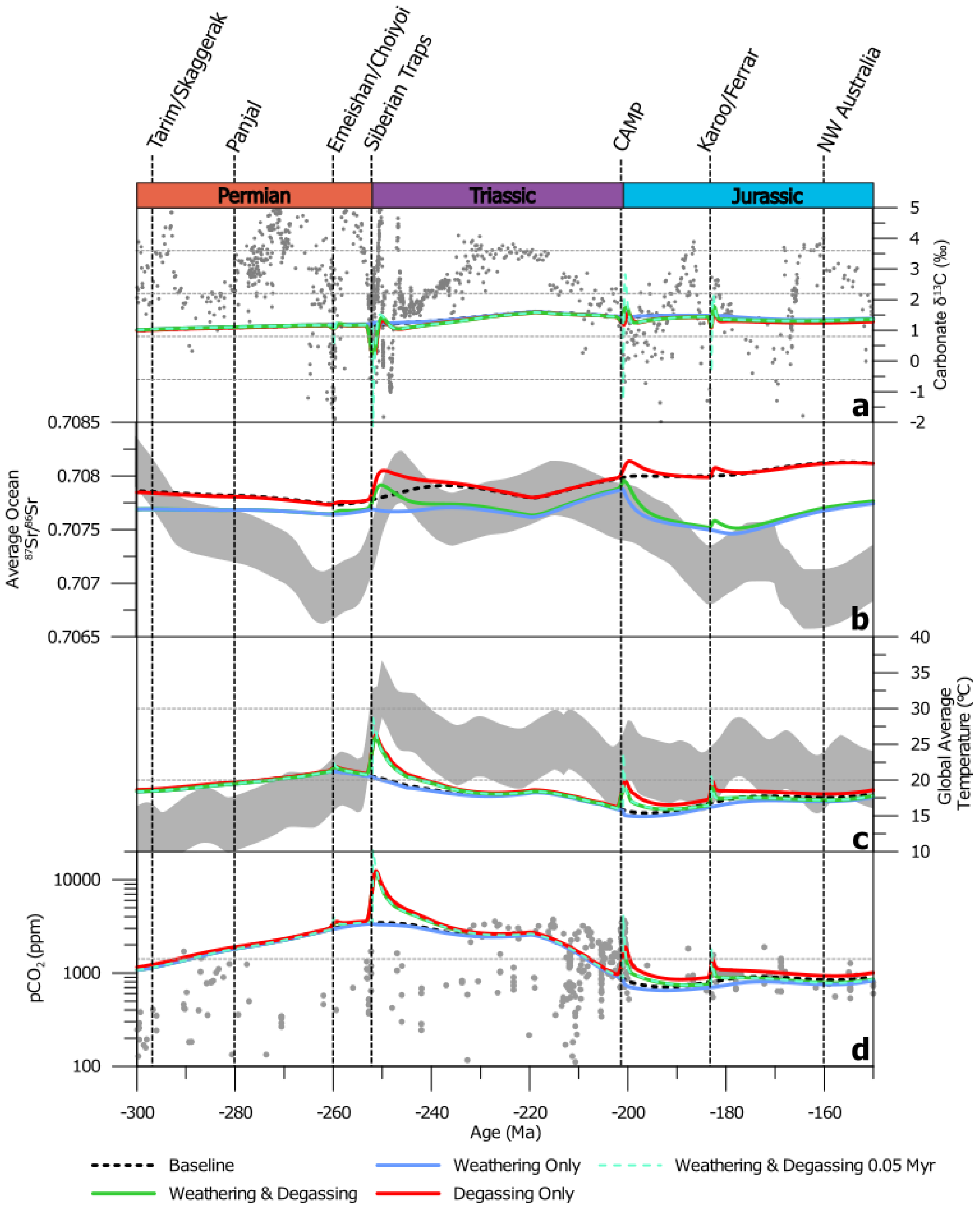

Figure 4 | Comparison of model outputs for five different scenarios. The upper panel displays the model-derived estimates of changing carbon isotope composition, with proxy reconstructions in grey circles. Below is reconstructed oceanic Sr isotope composition (solid lines) compared to oceanic Sr isotope proxy data (grey shaded area). The third panel shows reconstructed Global Average Temperature (solid lines) compared to reconstruction based on proxy data (grey shaded area). The final panel shows reconstructed atmospheric CO_2 levels (solid lines) compared to proxy measurements of CO2 (grey circles).